

Review

Kinetics of reduction of iron oxides by H₂ Part II. Low temperature reduction of magnetite

A. Pineau^{a,b,c,d,*}, N. Kanari^{a,b,c,d}, I. Gaballah^{a,b,c,d}

^a *Laboratoire Environnement et Minéralurgie, Rue du Doyen M. Roubault, BP 40, 54501 Vandœuvre Cedex, France*

^b *Centre National de la Recherche Scientifique, 3 Rue Michel-Ange, 75794 Paris Cedex, France*

^c *École Nationale Supérieure de Géologie, Rue du Doyen M. Roubault, BP 40, 54501 Vandœuvre Cedex, France*

^d *Institut National Polytechnique de Lorraine, 2 Rue de la Forêt de Haye, 54501 Vandœuvre Cedex, France*

Received 12 July 2006; received in revised form 10 January 2007; accepted 12 January 2007

Available online 20 January 2007

Abstract

This study deals with the reduction of Fe₃O₄ by H₂ in the temperature range of 210–950 °C. Two samples of Fe₃O₄ produced at 600 and 1200 °C, designated as Fe₃O₄₍₆₀₀₎ and Fe₃O₄₍₁₂₀₀₎, have been used as starting material.

Reduction of Fe₃O₄₍₆₀₀₎ by H₂ is characterized by an apparent activation energy ‘E_a’ of 200, 71 and 44 kJ/mol at $T < 250$ °C, 250 °C $< T < 390$ °C and $T > 390$ °C, respectively. The important change of E_a at 250 °C could be attributed to the removal of hydroxyl group and/or point defects of magnetite. This is confirmed during the reduction of Fe₃O₄₍₁₂₀₀₎. While transition at $T \approx 390$ °C is probably due to sintering of the reaction products as revealed by SEM.

In situ X-rays diffraction reduction experiments confirm the formation of stoichiometric FeO between 390 and 570 °C. At higher temperatures, non-stoichiometric wüstite is the intermediate product of the reduction of Fe₃O₄ to Fe.

The physical and chemical modifications of the reduction products at about 400 °C, had been confirmed by the reduction of Fe₃O₄₍₆₀₀₎ by CO and that of Fe₃O₄₍₁₂₀₀₎ by H₂. A minimum reaction rate had been observed during the reduction of Fe₃O₄₍₁₂₀₀₎ at about 760 °C. Mathematical modeling of experimental data suggests that the reaction rate is controlled by diffusion and SEM observations confirm the sintering of the reaction products.

Finally, one may underline that the rate of reduction of Fe₃O₄ with H₂ is systematically higher than that obtained by CO in the explored temperature range.

© 2007 Elsevier B.V. All rights reserved.

Keywords: Magnetite; Reduction; Hydrogen; Carbon monoxide; Low temperature

Contents

1. Introduction	76
2. Literature review	76
3. Material and experimental procedure	77
4. Results and discussion	78
4.1. Reduction of Fe ₃ O ₄₍₆₀₀₎ by hydrogen	78
4.2. Reduction of Fe ₃ O ₄₍₆₀₀₎ by CO	82
4.3. Reduction of Fe ₃ O ₄₍₁₂₀₀₎ by H ₂	84
4.4. Analysis of experimental results	85
5. Conclusions	87
Acknowledgments	87
References	88

DOI of original article: [10.1016/j.tca.2005.10.004](https://doi.org/10.1016/j.tca.2005.10.004).

* Corresponding author at: Laboratoire Environnement et Minéralurgie, Rue du Doyen M. Roubault, BP 40, 54501 Vandœuvre Cedex, France.

Tel.: +33 383 59 63 56.

E-mail address: Annye.Pineau@ensg.inpl-nancy.fr (A. Pineau).

1. Introduction

As mentioned in part I [1], more than 2 t of carbon dioxide are generated for the production of 1 t of iron metal. Low temperature study of the reduction of iron oxides with hydrogen may contribute to energy saving and low CO₂ emission. However, despite serious efforts [2–4], the cost of hydrogen production is currently high.

This paper is focused on the reduction of magnetite with hydrogen in the temperature range of 210–950 °C using thermogravimetric analysis (TGA) and a furnace allowing the ‘in situ’ X-rays diffraction. The objectives of this study are to

1. compare the reduction kinetic of Fe₃O₄, with hydrogen or carbon monoxide, with those of the reduction of hematite performed in part I;
2. confirm the presence of stoichiometric wüstite, at temperatures lower than 570 °C, as intermediate of the reduction of magnetite to iron using H₂;
3. explore the probable relation between the reactivity of magnetite and its initial physical characteristics by using two samples issued from pure hematite reduction by H₂–H₂O at 600 and 1200 °C;

4. check the eventual reduction kinetic’s modifications during the magnetite reduction and compare them with those of hematite reduction.

2. Literature review

Studies devoted to iron oxide reduction are abundant. Due to the industrial importance of this topic, extensive work had been done from the academic and applied point of view. However, results are contradictories as will be demonstrated below. This is because most authors use:

1. samples, either natural or pure, with different levels of impurities;
2. diverse experimental apparatus;
3. various temperature ranges;
4. distinctive gas mixtures with different levels of purity.

Consequently, the comparison of the reaction rate and the apparent activation energy ‘ E_a ’ obtained by different authors is impractical. Fig. 1 illustrates these contradictions. For instant, the reaction rate of the magnetite reduction, at the same temperature, can be different by several orders of magnitude. Moreover, Table 1a shows that E_a can vary from 13.4 to 167 kJ/mol.

Table 1a
Bibliographic survey of the effect of magnetite material on the apparent activation energy (kJ/mol) of its reduction by H₂ and suggested rate controlling process [5–16]

Material	Temperature range (°C)	Activation energy	Material, experimental conditions and kinetics controlling mechanism	Ref.
Natural and pure magnetite	200–280	60.6	Pure magnetite (0.5–3 μm), important interparticle diffusion phenomena	[9]
	234–450	77.7	Thin (89 μm) magnetite, chemical reaction, film mass-transfer effects (H ₂ , water vapor) above 450 °C, star-like pores in iron (smaller at higher temperatures)	[10]
	400–500	65.6	Magnetite crystals, abnormal low reduction rate above 500 °C: phenomenon of decrease in microporosity of the reduced layer	[11]
	400–500	72.1	Natural magnetite (2% SiO ₂), the area of the inner unreacted sphere is the rate controlling factor with the resistance diffusion of H ₂ , H ₂ O in metal	[6]
	390–580	86.0	Natural magnetite, reaction order $n = 1$	[12]
	325–600	69.3	Pure magnetite (99.95%), parabolic law of the degree of reduction $\alpha = (kt)^{0.5}$	[5]
	400–585	61.4	Disk and sheet samples, reduction rate controlled at Fe ₃ O ₄ –Fe interface	[13]
	585–900	13.4	Disk samples, reduction rate controlled at FeO–Fe interface, dense and stable FeO formed an protective layer	[13]
	910–1000	≈ or >62	Disk samples, abnormal increase in reduction rate (α to γ Fe transition)	[13]
	550–650	62.7	Briquettes of magnetite, phase boundary reaction	[8]
	800–1000	62.7 & 146.3	Briquettes of magnetite, 25–55% of reduction: $E_a = 62.7$ (phase boundary reaction), later stages of reduction $E_a = 146.3$ (diffusion of O ²⁻ ions in iron)	[8]
	1200–1300	68.6	Iron ore, Fe ₃ O ₄ → Fe	[14]
	Pellets	350–500	56.4	Dense Fe ₃ O ₄ , H ₂ pressure = 1–40 atm: as the H ₂ pressure increases, the reduction rate approaches a maximum rate: saturated surface with adsorbed H ₂ , phase boundary-controlled reaction (contracting sphere)
430–600		46	Magnetite pellets, controlling process at the hydrogen wüstite interface (interfacial gas-solid reaction)	[15]
900–1000		46	Magnetite pellets, controlling process at the hydrogen wüstite interface	[15]
700–900		≈167 or <167	Magnetite pellets, controlling process at the hydrogen wüstite interface and diffusion of iron in wüstite (solid state diffusion)	[15]
Above 570		57.1	Step Fe ₃ O ₄ → Fe, pellets containing fine magnetite and coal	[16]
Above 570		54.1	Step Fe ₃ O ₄ → FeO, pellets containing fine magnetite and coal	[16]
1200–1300		68.6	Step Fe ₃ O ₄ → Fe, iron ore	[14]
1200–1300		61.5	Step Fe ₃ O ₄ → FeO, iron ore	[14]

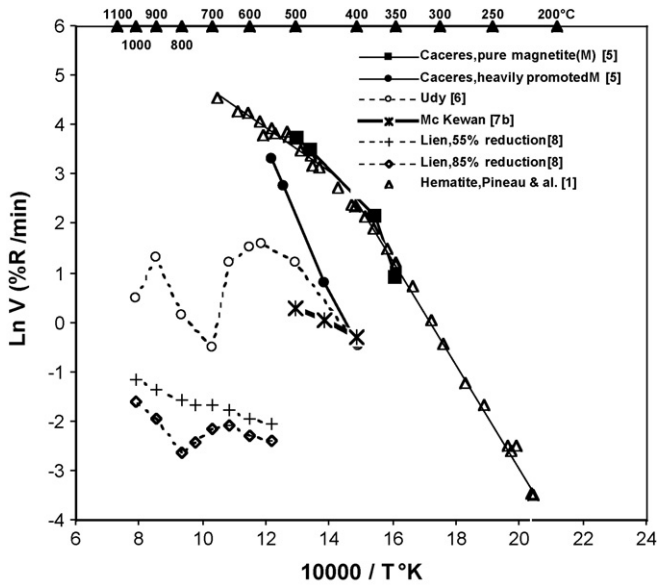


Fig. 1. Arrhenius diagrams for the reduction of magnetite by hydrogen.

Table 1b compares the E_a of the magnetite reduction using different gas mixtures as well as the controlling rate step as suggested by different authors. Again, using the same gas mixture for the magnetite reduction gives different apparent activation energies that are more or less related to the explored temperature range and the samples initial characteristics. As could be expected, the use of different gas mixtures leads to different values of E_a . However, the E_a values, for the reduction of Fe_3O_4 by different reducing gas mixtures, are more or less equivalents.

Several authors have found that the rate of magnetite reduction decreases or increases as function of the reaction

temperature [6,8,11,13,15,19]. They attributed this increase or decrease of the reaction rate to different physical modifications as summarized in Table 2.

Lien et al. [8] related the variations of the reduction rate to imperfections of the crystal lattices either as default or impurities. Colombo et al. [20] demonstrated that micro-deformation and defaults introduced by mechanical treatment of magnetite are eliminated by a thermal treatment at 500°C [21,22]. They also mentioned that H_2O associated to magnetite is removed at about 600°C . On the other hand, it is well known that the reaction rate of the gas-solid interaction could increase or decrease as solids are subjected to first or second-order transitions. This phenomenon is known as Hedvall effect [23–25].

Thus, the reactivity of iron oxides could be affected by the level of impurities, the extent of crystal defaults, the composition of the gas mixture and eventual phase transitions. In order to avoid the effect of impurities relatively pure sample of hematite had been used for the synthesis of magnetite used in this study. The reducing gas mixture is relatively pure and had a constant composition. On the other hand, two samples of Fe_3O_4 produced at 600 and 1200°C have been used as starting material to verify the eventual effect of crystal defaults on their reactivity.

3. Material and experimental procedure

The magnetite used in this study is obtained by the reduction of hematite supplied by Merck using a H_2 – H_2O gas mixture of adequate composition. Two samples are synthesized at 600 and 1200°C and designed as $\text{Fe}_3\text{O}_4(600)$ and $\text{Fe}_3\text{O}_4(1200)$. Their crystal parameter is 8.395 \AA . The grain size of $\text{Fe}_3\text{O}_4(600)$ is about $1\text{--}2 \mu\text{m}$ and its apparent specific surface area is $0.7 \text{ m}^2/\text{gr}$. While the grain size of $\text{Fe}_3\text{O}_4(1200)$ is $10\text{--}20 \mu\text{m}$ and its specific surface area is about $0.1 \text{ m}^2/\text{g}$.

Table 1b

Bibliographic survey of the effect of gas mixture on the apparent activation energy (kJ/mol) of the reduction of Fe_3O_4 and suggested rate controlling process [5,7b,12,14–18]

Gas mixture	Temperature range ($^\circ\text{C}$)	Activation energy	Material and experimental conditions and kinetics controlling mechanism	Ref.
H_2 – H_2O – N_2	400–500	56.8	Dense Fe_3O_4 , reduction rate approaches zero at magnetite/wüstite equilibrium, phase boundary-controlled reaction (contracting sphere)	[7b]
H_2	490–700	85.8	Synthetic magnetite + catalysts (SiO_2 , Al_2O_3 , CaO , MgO , K_2O), the reduction is shifted towards higher temperatures relatively to pure magnetite	[12]
	450–650	46.5	Commercial synthetic Fe_3O_4 + a few catalysts (SiO_2 , Al_2O_3 , CaO , MgO , K_2O)	[12]
	325–600	88.3	Slightly promoted magnetite: 2.2% of SiO_2 + MgO + CaO + Al_2O_3 + ...	[5]
	325–600	117.7	Heavily promoted magnetite: 7.8% of CaO + Al_2O_3 + SiO_2 + MgO + ...	[5]
	430–1000	46.0	Magnetite pellets and B_2O_3 , solid state diffusion of ferrous ions is increased by trivalent ions (bore) soluble in wüstite	[15]
CO	600–900	78.2	$\text{Fe}_3\text{O}_4 \rightarrow \text{FeO}$ in (porous) Fe_2O_3 reduction, shrinking occur during reduction	[17]
	600–900	64.4	$\text{Fe}_3\text{O}_4 \rightarrow \text{FeO}$ in Fe_3O_4 reduction, shrinking occur during reduction	[17]
	Above 570	69.6	$\text{Fe}_3\text{O}_4 \rightarrow \text{FeO}$, pellets containing fine magnetite and coal, chemical reaction and mixed control with Boudouard reactions	[16]
	Above 570	76.9	$\text{FeO} \rightarrow \text{Fe}$, pellets containing fine magnetite and coal	[16]
	1200–1300	65.7	$\text{Fe}_3\text{O}_4 \rightarrow \text{FeO}$, iron ore	[14]
	1200–1300	69.7	$\text{FeO} \rightarrow \text{Fe}$, iron ore	[14]
$\text{CO} + \text{CO}_2$	800–1050	121.2	$\text{Fe}_3\text{O}_4 \rightarrow \text{Fe}$, iron ore	[14]
			50% CO_2 , step $\text{Fe}_3\text{O}_4 \rightarrow \text{FeO}$, step-wise reduction of hematite pellets	[18]

Table 2
Variations of reaction rate in the range 600–700 °C during the reduction of Fe₃O₄ by H₂

Raw material	Temperature range (°C) of decreasing reaction rate and explanation	Temperature range (°C) of increasing reaction rate and explanation	Ref.
Synthetic magnetite	585–592: dense and stable wüstite forms a protective layer over Fe ₃ O ₄ surface	600–900: porous wüstite formed is non-protective	[13]
Magnetite crystals	Above 500: decrease in microporosity of the reduced layer	600–900, for 20–40% of reduction; decrease of reduction rate after 40% of reduction due to the drop of ultra- and microporosity of the reduction products	[11]
Briquettes of Fe ₃ O ₄ sintered at 1200 °C	650–800: presence of a secondary reaction zone: individual wüstite crystals into the iron band (solid-state diffusion through the recrystallized iron surrounding the individual wüstite crystals - crystal imperfections of iron are removed). Certain impurities in the lattice of iron oxides cause an increase in the number of imperfections and eliminate the rate minimum	800–1000: during the earlier stages of reduction (25–55%), phase boundary reaction (rapid diffusion of ions through the large number of crystals defects and imperfections in the newly formed wüstite and iron phases). In the later stages (85% of reduction): solid-state diffusion	[8]
Magnetite concentrate	600–700: sintering and consolidation of a shell of metallization advances from the outside of grain toward the interior with increasing time, the metal jacket resists to penetration by H ₂ and especially by water vapor. Sintering is greatly enhanced by the presence of sulfides and silica	700–1000: restoration of diffusion	[6]
Magnetite, 4% SiO ₂ , 4% Al ₂ O ₃	600–700 and 700–800 for later stages of reduction: lagging phenomenon due to entrapped H ₂ O, the factor responsible for lagging has the nature of a protective envelope, either the metallic Fe itself or a nonmetallic film	700–800 for previous stages of reduction: the trapped gaseous phase at high internal pressures is able to burst the enclosing film, disruption of the metallic shell destroys the metastable equilibrium conditions and the reduction proceed again	[19]
Pure magnetite pellets	About 700–900: control of reduction is increasingly interfered by diffusion of iron in wüstite and solid-state reaction, a substantial retention (50%) of wüstite in the iron occurs at 700 °C, the retained wüstite becomes progressively coarser and its amount less from 700 to 900 °C	At 900 °C, islands of wüstite diminish in size towards the outside of the specimen	[15]
Pure magnetite pellets with controlled amount of B ₂ O ₃	Increasing rate of reduction at all temperatures: the rate of solid-state diffusion of ferrous ions in wüstite is increased by the presence of the soluble trivalent bore ions that is soluble in wüstite, the reduction proceeds with the formation of discrete layers of reaction products. Contrarily, the rate of reduction is decreased when trivalent (Al, Cr) ions insoluble in wüstite are present in wüstite		[15]

Thermogravimetric analysis tests were performed using 100 mg of the sample and a Cahn microbalance. The experimental protocol and the details of this apparatus are described in part I of this paper.

'In situ' reduction of magnetite was carried out using an X-rays furnace. This furnace allows automatic data collection of formed solids for $\theta = 0\text{--}60^\circ$. The goniometer speed was adapted to the reaction kinetics at different temperatures and varied from $\theta = 0.25^\circ$ to $1^\circ/\text{min}$.

Raw samples and reaction products are systematically examined by X-rays diffraction (XRD), scanning electron microscope (SEM) and eventually by chemical analysis.

4. Results and discussion

4.1. Reduction of Fe₃O₄₍₆₀₀₎ by hydrogen

Fig. 2 groups the isotherms of this magnetite reduction versus the reaction time at different temperatures. These isotherms have the sigmoid form. For a reduction extent (%R = weight loss \times 100/27.64) of 50%, the reaction duration

is about 500, 140, 11 and 3 min at 239, 258, 352 and 426 °C, respectively.

The Arrhenius diagram traces the evolution of $\ln V$ versus $1/T$ (°K) as shown by Fig. 3. At temperatures lower than 250 °C, E_a is about 200 kJ/mol. It decreases to about 71 kJ/mol for the temperature range 250–390 °C. At temperatures higher than 390 °C, E_a is equal to 44 kJ/mol.

The important change of the E_a value around 250 °C could be attributed to

1. a modification of the physical characteristic of the generated iron in this temperature range;
2. the suppression or the modification of configuration of point defects of Fe₃O₄₍₆₀₀₎ [26];
3. change of status of H₂O associated to the magnetite [27–30];
4. low flow rate of the reducing gas mixture leading to starvation and decrease of the reaction rate.

The first hypothesis can be considered as several authors [31–33] have observed a peak of internal friction of iron at about 250 °C. The second hypothesis is confirmed by several authors

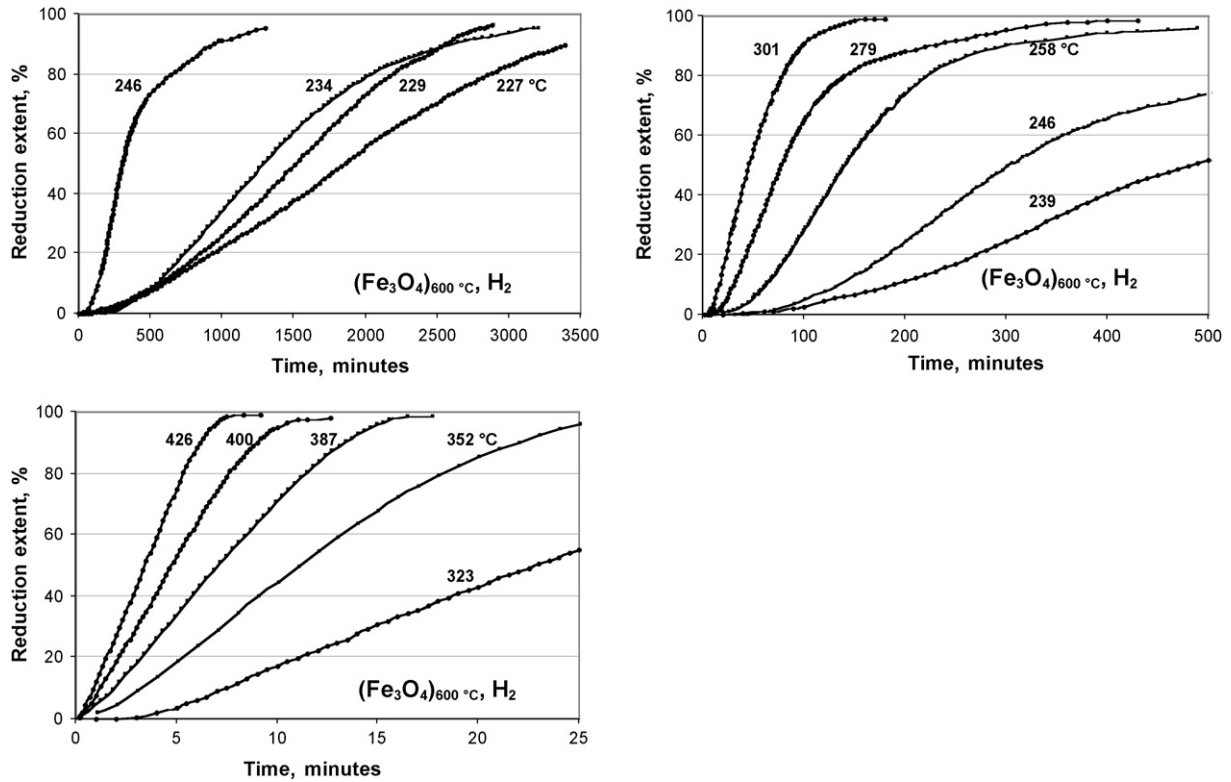


Fig. 2. Evolution of reduction extent vs. reaction time for the reduction of $\text{Fe}_3\text{O}_4(600)$ with hydrogen.

[34–36] during the oxidation of magnetite. These authors used differential thermal analysis ‘DTA’ and found an exothermic peak at $250 \pm 20^\circ\text{C}$ during the oxidation of magnetite. They contributed this peak to the formation of $\gamma\text{-Fe}_2\text{O}_3$. However, Behar and Collongues [37] found that disordered $\gamma\text{-Fe}_2\text{O}_3$, prepared at low temperatures, is well ordered at 250°C .

The third hypothesis based on the consideration that the oxygen of magnetite, prepared at $T \leq 600^\circ\text{C}$, could be replaced by OH^- ions [27–29]. This had been confirmed by Colombo et al. [20] as they found that magnetite loses its associated water at temperatures higher than 600°C . This could be related to our experimentation for the unsuccessful preparation of magnetite at 400°C . This is because the prepared magnetite using $\text{H}_2\text{-H}_2\text{O}$ gas mixture, at this temperature, is pyrophoric in contact with air. Thus one should expect that reduction of magnetite, prepared at 1200°C , should not exhibit any anomaly at 250°C due to the elimination of protons and/or hydroxyl groups at $T > 600^\circ\text{C}$. This will be examined in the next paragraph.

The fourth hypothesis cannot be considered as the increase of the flow rate from 100 to 300 l/h does not augment the reaction rate.

One may conclude that the first hypothesis can be excluded as the anomaly at 250°C is experienced for the reduction and oxidation of magnetite. Thus this anomaly is probably due to intrinsic property of magnetite. The second and third hypothesis can be validated by considering that the association of protons and/or the hydroxyl group to point defects that are modified at about 250°C .

The mathematical modeling of the experimental data of Fig. 2 is presented in Fig. 4. The models used are summarized in Table 3. Eqs. (1)–(12) covers most of the probable mechanisms that controls the gas–solid reactions. At temperatures lower than 400°C , Fig. 4 suggests that the reaction rate is controlled by phase boundary according to Eq. (3) or Eq. (4). At temperatures higher than 390°C , Eq. (11) seems to fit the experimental data.

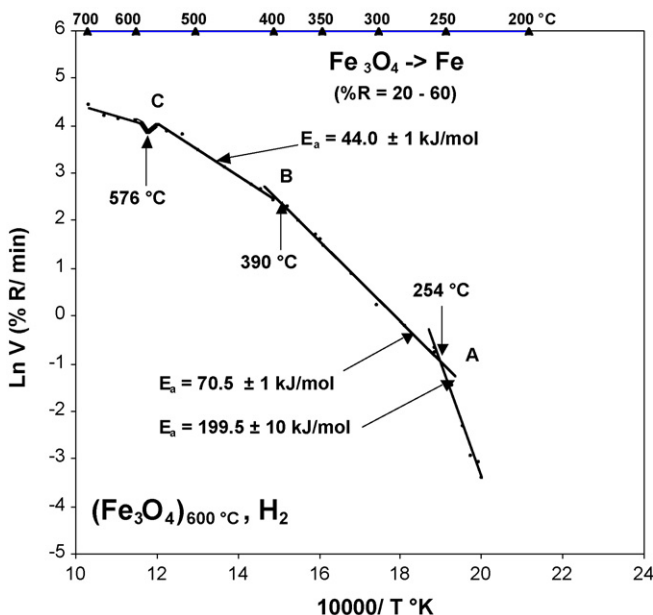


Fig. 3. Arrhenius diagram for the reduction of $\text{Fe}_3\text{O}_4(600)$ by hydrogen.

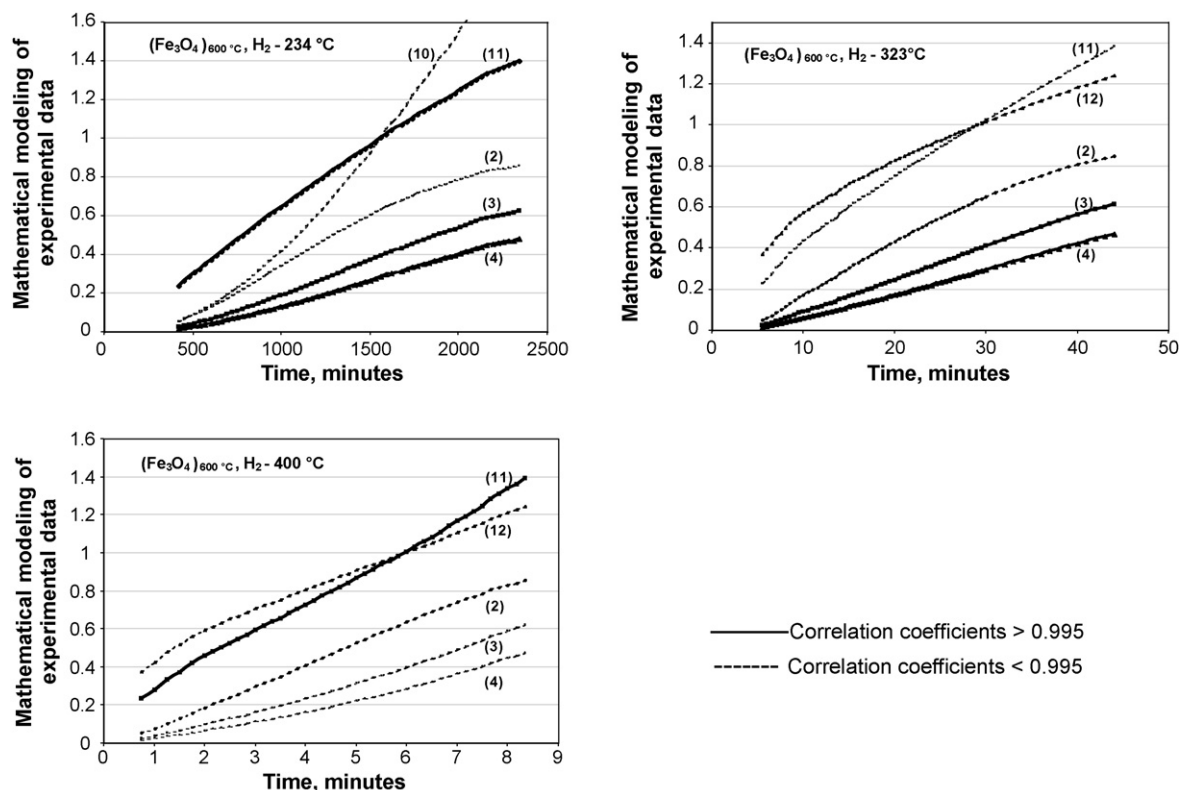


Fig. 4. Mathematical modeling of experimental data of Fig. 2.

This equation suggests that the reaction rate is controlled by two-dimensional growth of nuclei.

The morphological aspects of $\text{Fe}_3\text{O}_{4(600)}$ and the evolution of the reduced magnetite versus the temperature are grouped in Fig. 5. It seems that there are no morphological modifications of the reaction products reduced at temperatures lower than 390°C (pictures A–C). However, at temperatures higher than 390°C , the grain size of the reaction product increased demonstrating their sintering. This suggests that there is a physical modifica-

tion of the reduction products occurs around 390°C designed as transition temperature ' T_1 '.

To check this hypothesis, in situ X-rays diffraction experimentation of the reduction of $\text{Fe}_3\text{O}_{4(600)}$ by H_2 in the temperature range of 250 – 700°C had been performed. Eq. (13) summarizes the obtained results.

At temperature lower than 390°C , magnetite is reduced directly to iron. Between 390 and 570°C , reduction of magnetite passes by an intermediate that is the wüstite before the

Table 3
Suggested mathematical modeling of reaction kinetics

Equation	Shape factor	Mechanism
$kt = 1 - (1 - X)^{1/F_p}$ (1)		General equation [38]
$kt = X$ (2)	1	Phase-boundary-controlled reaction (infinite slabs)
$kt = 1 - (1 - X)^{1/2}$ (3)	2	Phase-boundary-controlled reaction (contracting cylinder)
$kt = 1 - (1 - X)^{1/3}$ (4)	3	Phase-boundary-controlled reaction (contracting sphere)
$kt = X^2$ (5)	1	One-dimensional diffusion
$kt = X + (1 - X)\ln(1 - X)$ (6)	2	Two-dimensional diffusion
$kt = 1 - 3(1 - X)^{2/3} + 2(1 - X)$ (7)	3	Three-dimensional diffusion
$kt = \left[1 - \left(\frac{2}{3}X\right)\right] - (1 - X)^{2/3}$ (8)	3	Three-dimensional diffusion (Ginstling–Brounshtein equation) [39]
$kt = [1 - (1 - X)^{1/3}]^2$ (9)	3	Three-dimensional diffusion (Jander equation) [39]
$kt = [-\ln(1 - X)]$ (10)	1	Random nucleation; unimolecular decay law (first-order)
$kt = [-\ln(1 - X)]^{1/2}$ (11)	2	Two-dimensional growth of nuclei (Avrami–Erofeyev equation)
$kt = [-\ln(1 - X)]^{1/3}$ (12)	3	Three-dimensional growth of nuclei (Avrami–Erofeyev equation)

where, k = constant, t = reduction time, X = extent of reduction ($X = 0$ at the beginning of the reduction and $X = 1$ at the end of reduction), F_p = particle shape factor (1 for infinite slabs, 2 for long cylinders, and 3 for spheres).

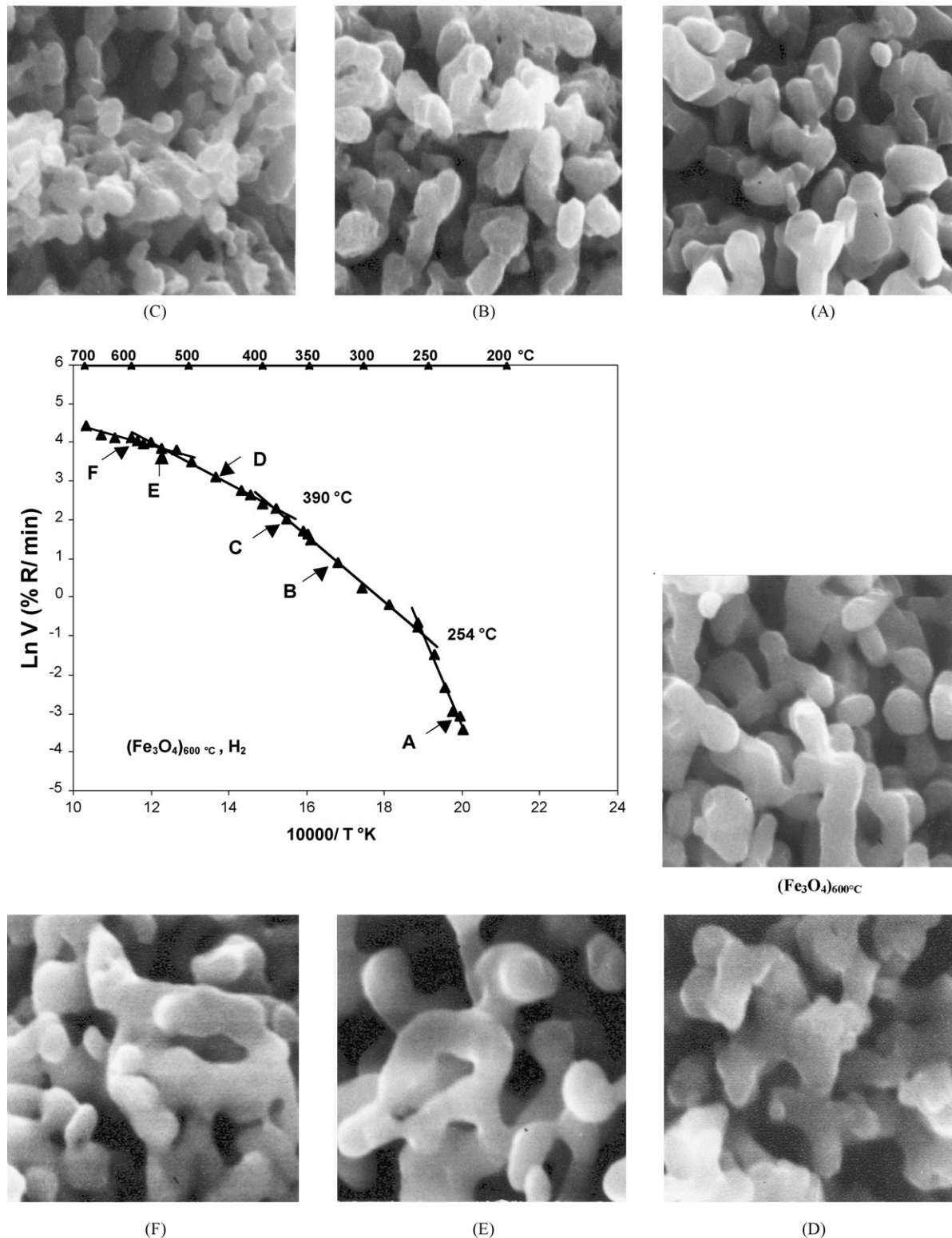


Fig. 5. Evolution of morphological aspects of the reduction products of $\text{Fe}_3\text{O}_4(600)$ vs. the temperature ($X = 10\,000 \pm 1000$).

formation of iron. The crystal parameter of this wüstite is about 4.33 Å confirming the formation of stoichiometric FeO. At temperatures higher than 570 °C, the reduction of magnetite proceeds through the formation of non-stoichiometric wüstite.

It seems that the decrease of E_a around 390 °C is related to the formation of stoichiometric wüstite during the reduction of $\text{Fe}_3\text{O}_4(600)$ with H_2 . This behavior is similar to that of the reduction of hematite with hydrogen around 420 °C [1]. To check whether this behavior is related to the nature of the

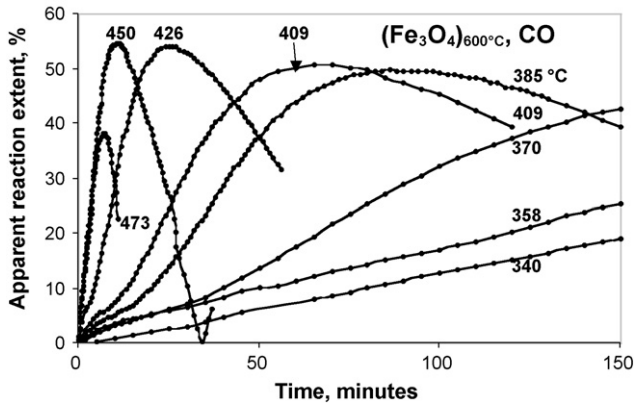


Fig. 6. Evolution of reduction extent vs. reaction time for the reduction of $Fe_3O_{4(600)}$ with CO.

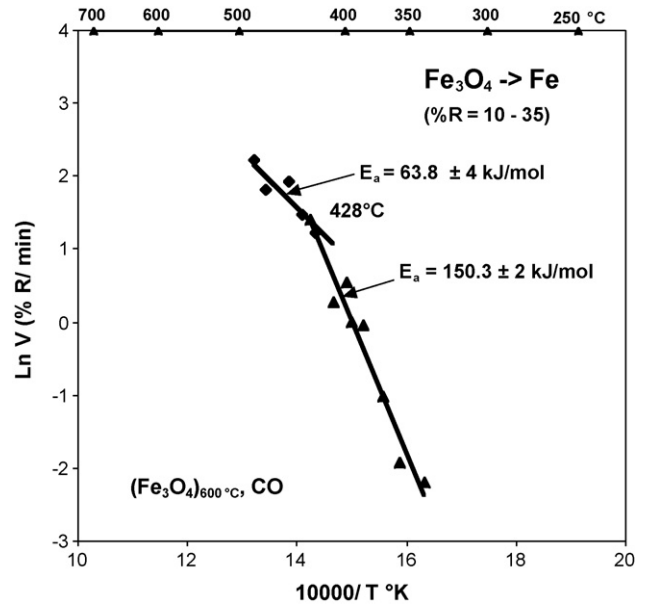
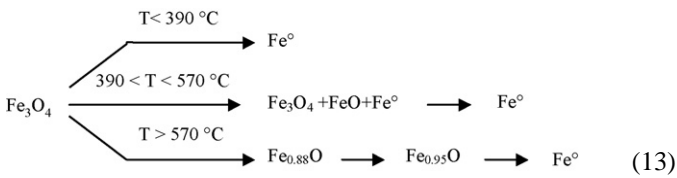


Fig. 7. Arrhenius diagram for the reduction of $Fe_3O_{4(600)}$ by CO.

reducing gas or to the intrinsic physical properties of magnetite, reduction of $Fe_3O_{4(600)}$ with CO was studied between 300 and 500 °C.



4.2. Reduction of $Fe_3O_{4(600)}$ by CO

Fig. 6 shows the isotherms of the magnetite reduction with carbon monoxide. The decrease and the increase of the sample weight is due to the reduction of magnetite in iron followed

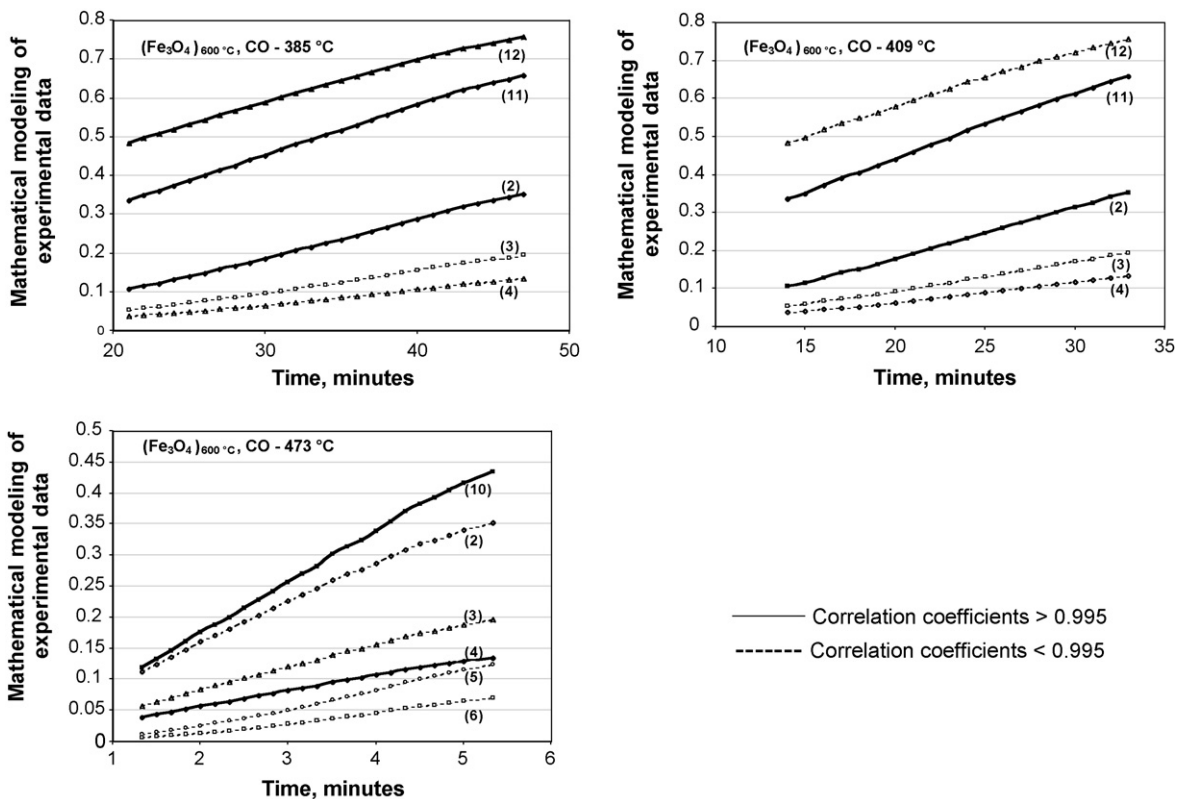


Fig. 8. Mathematical modeling of experimental data of Fig. 6.

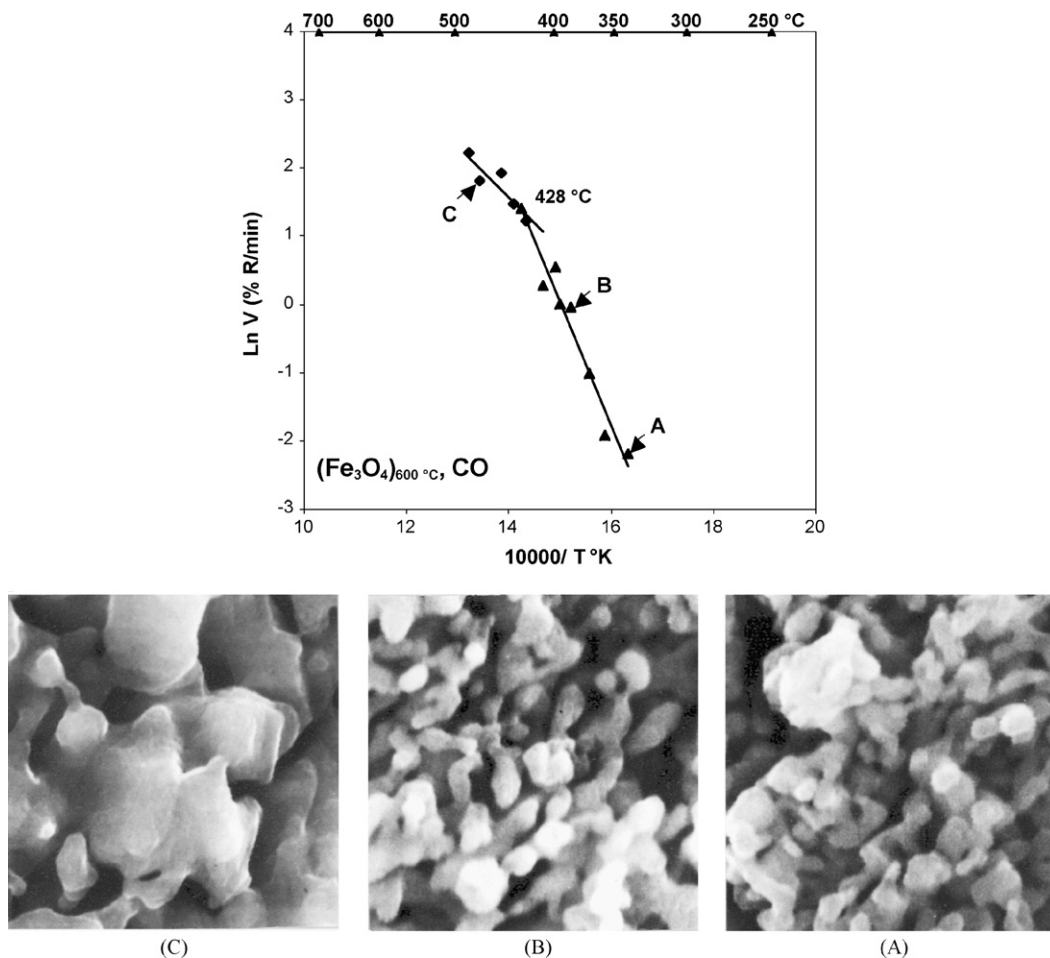


Fig. 9. Morphological aspects of reduced $\text{Fe}_3\text{O}_4(600)$ by CO at different temperatures ($X = 7000 \pm 700$).

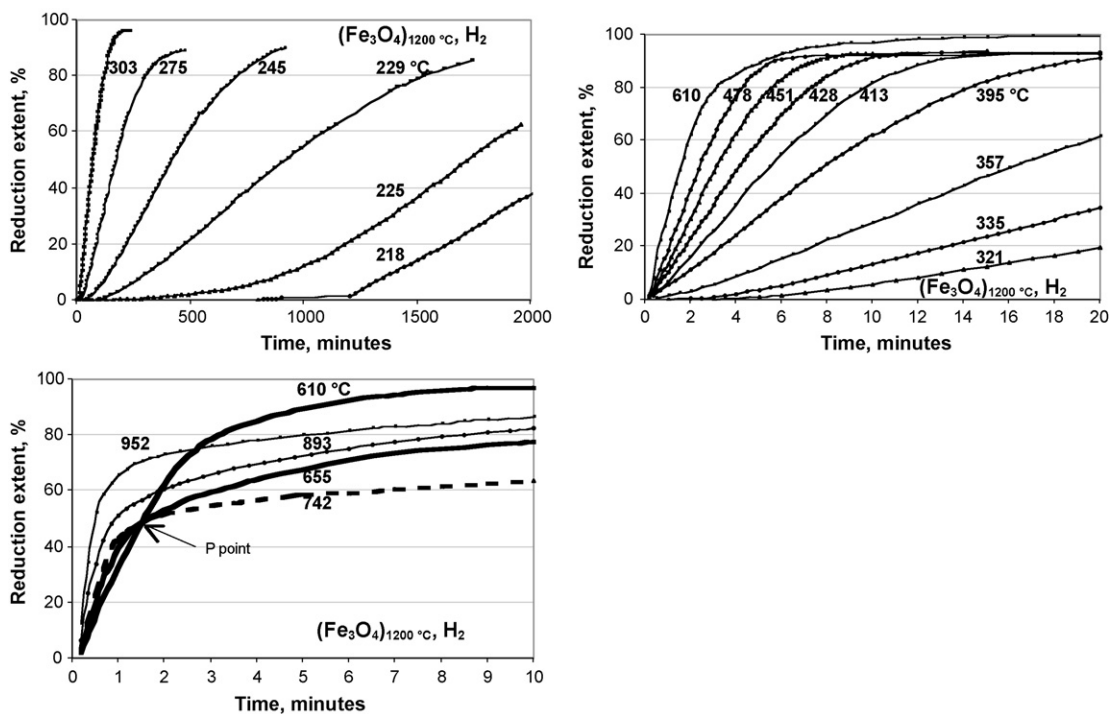


Fig. 10. Evolution of reaction extent vs. reaction time for the reduction of $\text{Fe}_3\text{O}_4(1200)$ with H_2 .

by the formation of iron carbide resulted from the decomposition of carbon monoxide. Only the beginning of the isotherm ($%R = 10\text{--}35$) is employed for the construction of the Arrhenius diagram as shown by Fig. 7. This figure indicates a decrease of E_a from 150 to 64 kJ/mol at temperatures lower and higher than 428 °C, respectively.

Mathematical modeling of experimental data of Fig. 6 is grouped in Fig. 8. At temperatures lower than 430 °C, the reaction rate is controlled by two and/or three-dimensional nuclei growth. At higher temperature, diffusion controls the reaction rate. Fig. 9 exhibits some of the morphological aspects of the reduction products. This figure suggests that sintering occurs at temperatures higher than 430 °C.

One may underline that the transition temperatures for the reduction of magnetite by H_2 and CO are comparables. It seems that the kinetic modification is related to the intrinsic physical properties of magnetite.

To confirm this hypothesis, reduction of $Fe_3O_{4(1200)}$ by hydrogen is performed between 210 and 950 °C.

4.3. Reduction of $Fe_3O_{4(1200)}$ by H_2

Fig. 10 groups the isotherms of reduction of magnetite at different temperatures. This figure shows that at temperatures lower than 600 °C, the isotherms have the traditional sigmoid form. While at temperatures higher than 600 °C, the sigmoid form of isotherms is replaced gradually by the parabolic one.

Fig. 11 groups the Arrhenius diagrams for different reduction extent of $Fe_3O_{4(1200)}$ by H_2 . This figure suggests that for a reduction extent of

1. 5–20%, E_a decreases from 77 to 27 kJ/mol for temperatures lower and higher than 450 ± 10 °C (Fig. 11A);
2. 20–60%, E_a decreases at temperatures higher than 390 ± 5 °C and the reduction rate passes by a maximum at about 577 ± 5 °C. Starting at about 600 °C, the reaction rate decreases to attain a minimum at 766 ± 5 °C. Between 770 and 950 °C, the reduction rate increases with a discontinuity at around 900 °C (Fig. 11B);

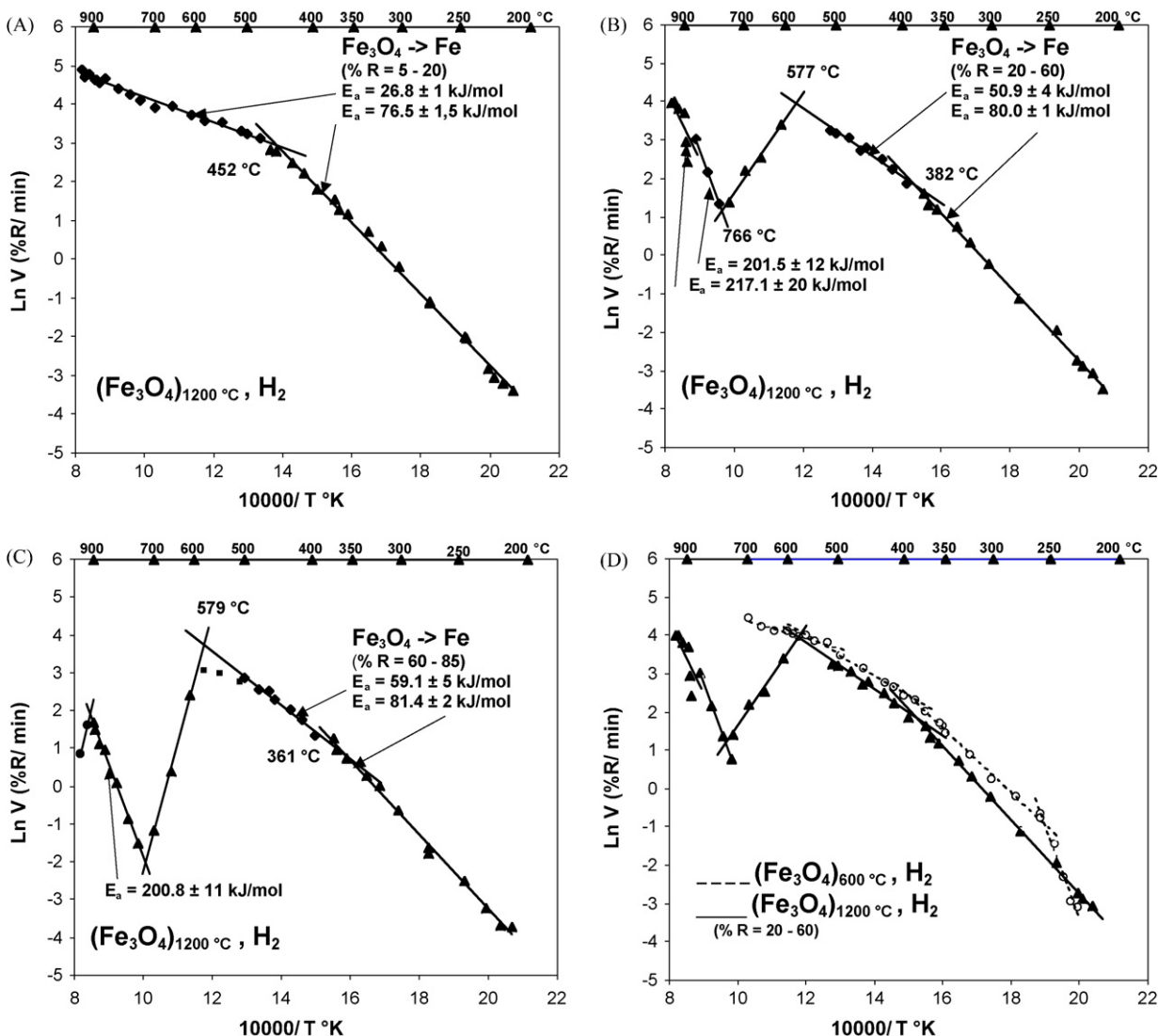


Fig. 11. (A–D) Arrhenius diagrams for the reduction of $Fe_3O_{4(1200)}$ by H_2 .

- 60–85%, the evolution of the reaction extent is identical to that described in 2 (Fig. 11C).

Fig. 11D compare the Arrhenius diagrams for the reduction of $\text{Fe}_3\text{O}_4(600)$ and $\text{Fe}_3\text{O}_4(1200)$ for a reaction extent of 20–60%. One may underline:

- the modification of the reaction rate at 250 °C observed during the reduction of $\text{Fe}_3\text{O}_4(600)$ does not exist during the reduction of $\text{Fe}_3\text{O}_4(1200)$;
- between 250 and 500 °C, the reaction rates of the two magnetite are comparables;
- at temperatures higher than 600 °C, the reaction rate of $\text{Fe}_3\text{O}_4(1200)$ decreases while that of $\text{Fe}_3\text{O}_4(600)$ increases.

Fig. 12 groups the mathematical modeling of experimental data shown in Fig. 10 at 357, 478 and 878 °C. This figure suggests that the reduction rate for 357 and 478 °C is controlled by phase boundary according to Eqs. (3) and (4). At 878 °C, it seems that Eq. (6) is the best fit for the experimental data. It indicates that the reaction rate is controlled by diffusion.

Fig. 13 exhibits the evolution of the morphological aspects of the reaction product of the $\text{Fe}_3\text{O}_4(1200)$ reduction versus the reaction temperature. The photos A–C of this figure show a start like bursts. The size of these stars decreases as temperature increases while their number increases. Photos D and E, obtained at temperatures higher than 700 °C, confirm the sintering of the reaction products as compared to the initial sample.

One may underline that the comparison between Figs. 5 and 13 indicates that the grain size of $\text{Fe}_3\text{O}_4(1200)$ is bigger than that of $\text{Fe}_3\text{O}_4(600)$. For both samples, the reaction products of the magnetite reduction are agglomerated and begin at temperatures higher than 400 °C.

Finally Fig. 14 compares the Arrhenius diagrams of the reduction of hematite and $\text{Fe}_3\text{O}_4(1200)$. At temperatures lower than 400 °C, the rates of reaction of the two solids are almost identical. However, at temperatures higher than 600 °C, the behavior of the two solids is different.

One may underline that the kinetic modifications observed at about 250 °C during the reduction of $\text{Fe}_3\text{O}_4(600)$ does not exist for both solids. This is probably due to absence of point defects that are eliminated during the synthesis or the purification of these solids at high temperature.

4.4. Analysis of experimental results

The results of different series of experiments and the above discussion confirm that the kinetic modification of the reduction rate could be affected by point defects and/or crystal defaults depending on the temperature range of the reduction of iron oxides. This is because:

- The kinetic modification of the reduction rate, around 400 °C, occurs for both $\text{Fe}_3\text{O}_4(600)$ and $\text{Fe}_3\text{O}_4(1200)$.
- Use of H_2 or CO as reducing gas, does not affect the kinetic modification at ≈ 400 °C.

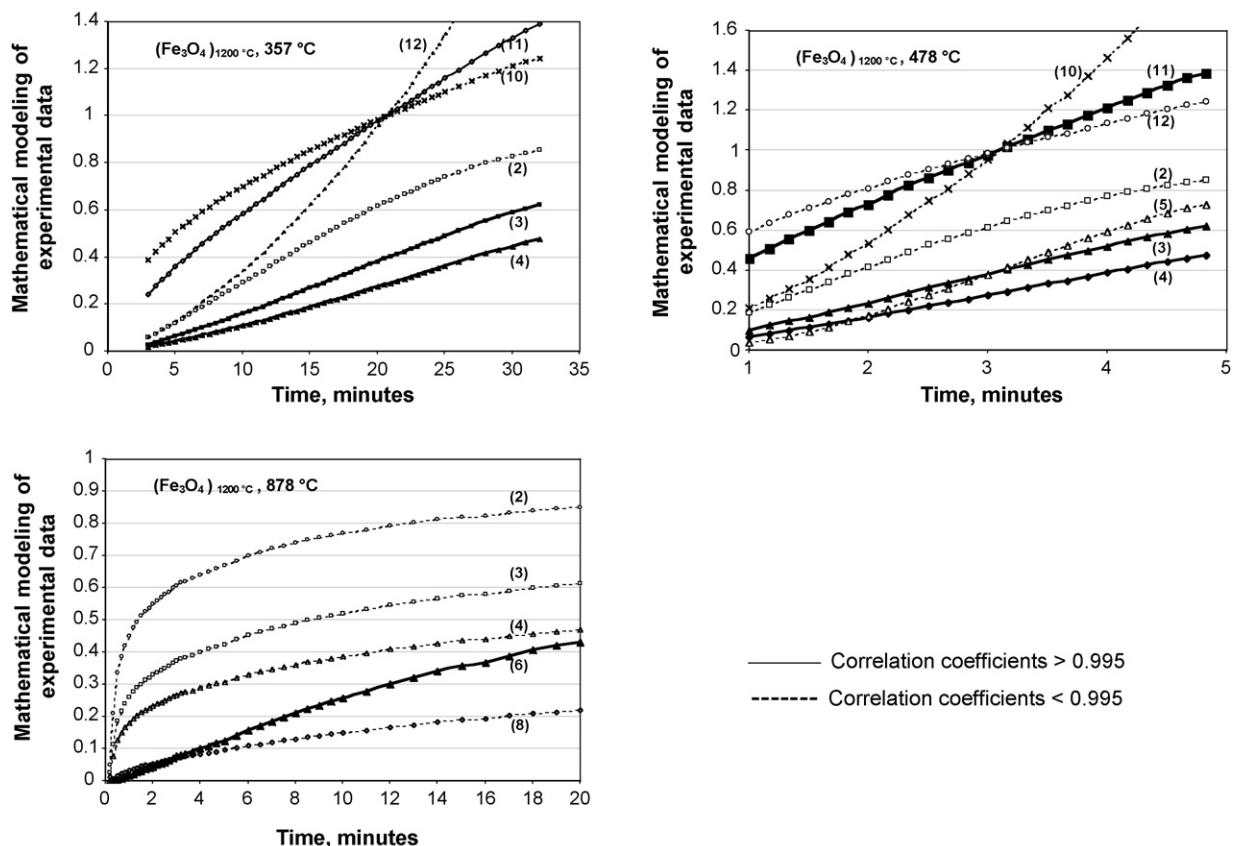


Fig. 12. Mathematical modeling of experimental data of Fig. 10.

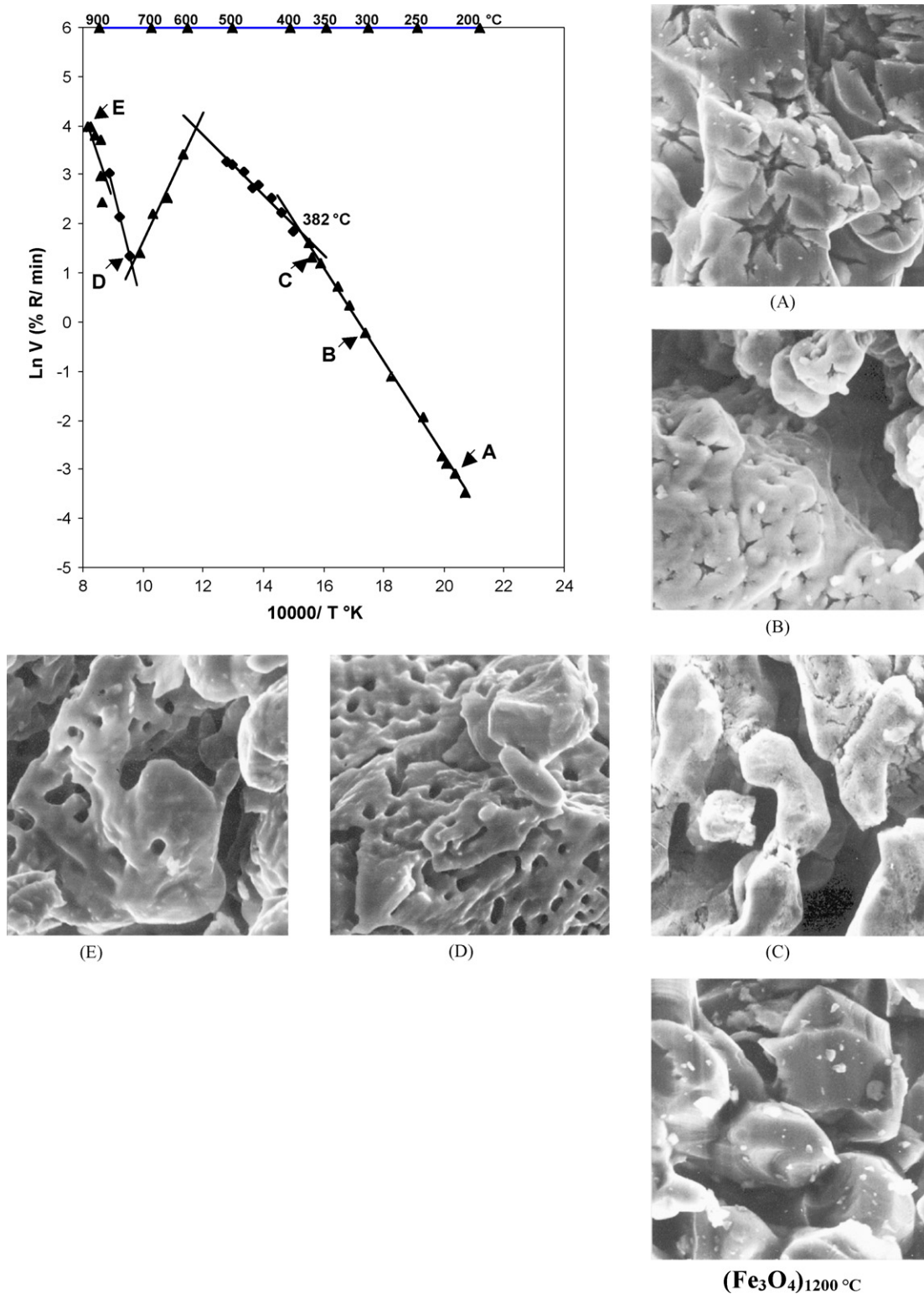


Fig. 13. Evolution of morphological aspects of the reduction products of $\text{Fe}_3\text{O}_4(1200)$ by hydrogen at different temperatures ($X = 1500 \pm 150$).

3. Increasing the flow rate of the reducing gas does not change this modification.
4. The kinetic modification at 250°C occurs only during the reduction of $\text{Fe}_3\text{O}_4(600)$. This is probably due to the presence of point defects or water in the magnetite structure prepared at relatively low temperature.
5. The agglomeration of the reduction products starts at temperatures $> 400^\circ\text{C}$.
6. The formation of stoichiometric wüstite, during the reduction of Fe_2O_3 and Fe_3O_4 is proved only in the temperatures range $450\text{--}570^\circ\text{C}$. This could be attributed to better crystal structure due to the annealing of defaults.

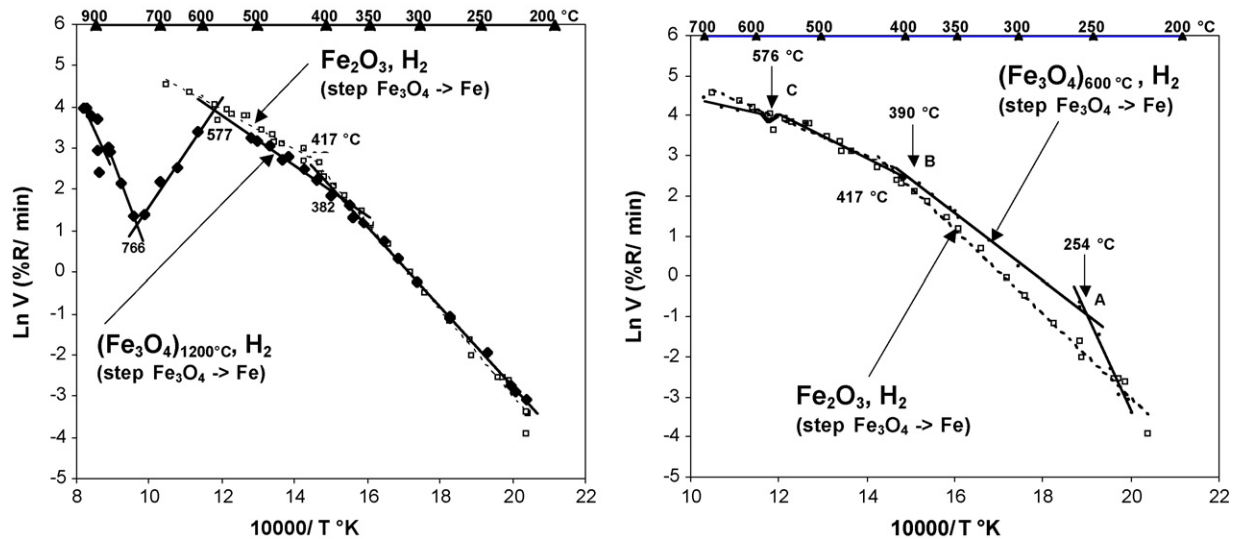


Fig. 14. Comparison of the Arrhenius diagrams for the reduction of Fe_2O_3 and Fe_3O_4 by H_2 .

- The phenomenon of the minimum of the reaction rate, at $T \approx 750^\circ\text{C}$, occurs only during the reduction of $\text{Fe}_3\text{O}_4(1200)$. This tends to confirm that the severe sintering of the reduction product is responsible of this behavior.

5. Conclusions

Results of the reduction of two samples of Fe_3O_4 prepared at 600 and 1200 °C [$\text{Fe}_3\text{O}_4(600)$ and $\text{Fe}_3\text{O}_4(1200)$] with hydrogen in the temperature range of 210–950 °C leads to the following conclusions:

- The Arrhenius diagram presents two modifications of E_a at 250 and at 390 °C. The apparent activation energy E_a decreases from 200 kJ/mol to about 71 kJ/mol between 250 and 390 °C. At higher temperatures E_a falls to 44 kJ/mol.
- These kinetic modifications could be related to the intrinsic physical properties of Fe_3O_4 and/or reduction products.
- The kinetic modification at 250 °C is not observed during the reduction of $\text{Fe}_3\text{O}_4(1200)$. This is probably due to the annealing of point defects during the synthesis of this magnetite.
- It seems probable that the kinetic modifications of the reduction rate at about 380–420 °C, during the reduction of $\text{Fe}_3\text{O}_4(600)$, $\text{Fe}_3\text{O}_4(1200)$ and Fe_2O_3 , to the formation of stoichiometric FeO between 390 and 570 °C and to the agglomeration of the reduction products.
- The observed minimum reduction rate of $\text{Fe}_3\text{O}_4(1200)$ at about 760 °C seems to be related to severe sintering of the reduction product.
- At temperatures higher than 570 °C, the reduction of magnetite proceeds through the formation of non-stoichiometric wüstite.
- Mathematical modeling of experimental data, at temperatures lower than 430 °C, suggests that the controlling mechanism of the reaction rate is nucleation and/or phase

boundary reaction. At temperature higher than 430 °C for $\text{Fe}_3\text{O}_4(600)$ reduced with CO and higher than 650 °C for $\text{Fe}_3\text{O}_4(1200)$ reduced by H_2 , the controlling mechanism is diffusion.

- The reduction rate of Fe_3O_4 with H_2 is systematically higher than that obtained with CO in the explored temperature range.
- SEM's observations of the reduction products show their gradual agglomeration and sintering as the temperature increases. This leads to a decrease of E_a thus lowering the thermal efficiency of the reduction process.

From the practical point of view, one should emphasize that low temperature reduction of iron oxides with H_2 is handicapped by the cost of hydrogen production. On the other hand, the important decrease of E_a at temperatures higher than 400 °C suggests that the best energy efficiency is around this temperature. However, it is also in this temperature range that the pyrophoric character of the reduction products is manifested.

While results of this work outline the important role of point and linear defects on the reduction rate of iron oxides, one should underline the lack of data about the behavior of point and linear defects of iron oxides as function of temperature. The role exact of the protons and hydroxyl groups in the magnetite structure and their eventual association with the crystal defects is almost unknown. Research in this area could boost the large-scale low temperature reduction of iron oxides with hydrogen.

Acknowledgments

Part of this work was performed in 'Laboratoire de Chimie du Solide' of the University of Nancy, France and the Massachusetts Institute of Technology 'MIT', Dept. of Material sciences. The authors thank Prof. J. Szekely and Dr. Ch. Gleitzer for their help and discussions. They also indebted to Mrs. Ch. Richard for her kind help in technical and administration work.

References

- [1] A. Pineau, N. Kanari, I. Gaballah, *Thermochim. Acta* 447 (2006) 89.
- [2] Anonymous, Hydrogen production, in: US Climate Change Technology Program—Technology Options for the Near and Long Term, November, 2003, p. 75. Edited in Technology options, 2005. <http://www.climatscience.gov/library/>.
- [3] L. Barreto, A. Makihira, K. Riahi, *Int. J. Hydrogen Energy* 28 (2003) 267.
- [4] A. Carlson, *Energy Policy* 31 (2003) 951.
- [5] P.G. Caceres, M.H. Behbehani, *Appl. Catal. A: Gen.* 109 (2–3) (1994) 211.
- [6] M.C. Udy, C.H. Lorig, *TMS AIME* 154 (1943) 162.
- [7] (a) W.M. McKewan, *AIME Trans.* 224 (1962) 387;
(b) W.M. McKewan, *AIME Trans.* 221 (1961) 140.
- [8] H.O. Lien, A.E. El-Mehairy, H.U. Ross, *J. Iron Steel Inst.* 209 (1971) 541.
- [9] G. Liberti, G. Servi, A. Gaulio, C. Ruffino, N. Pernicone, *J. Therm. Anal.* 6 (1974) 183.
- [10] M.M. Al-Kahtany, Y.K. Rao, *Ironmak. Steelmak.* 7 (1980) 49.
- [11] G.I. Tschufarov, et al., *Acta Physicochim. (URSS)* 3 (1935) 957.
- [12] S.S. Bogdanov, B.D. Aleksii, I.G. Mitov, D.G. Klisurski, N.A. Petranovi, *Thermochim. Acta* 173 (27) (1990) 71.
- [13] M. Quets, M.E. Wadsworth, J.R. Lewis, *AIME Trans.* 218 (1960) 545.
- [14] S. Sun, W.-K. Lu, *ISIJ Int.* 39 (1999) 123.
- [15] V.J. Moran, A.E. Jenkins, *JISI* 199 (1961) 26.
- [16] P.C. Coetsee, E.E. Pistorius, de Villiers, *Miner. Eng.* 15 (11 suppl. 1) (2002) 919.
- [17] K.L. Trushenski, W.O. Philbrook, *Metall. Trans.* 5 (1974) 1149.
- [18] T. Murayama, Y. Ono, Y. Kawai, *Trans. Iron Steel Inst. Jpn.* 18 (1978) 579.
- [19] G. Specht Jr., C.A. Zaffe, *TMS AIME* 167 (1946) 237.
- [20] U. Colombo, F. Gazzarrini, G. Lanzavecchia, *Mater. Sci. Eng.* 2 (2) (1967) 445.
- [21] F. Gazzarini, G. Lanzavecchia, in: J.W. Mitchell, et al. (Eds.), *Proceeding of 6th ISRS*, Wiley Interscience, 1969, p. 57.
- [22] J. Fagherazzi, G. Lanzavecchia, *Mater. Sci. Eng.* 5 (2) (1970) 63.
- [23] J.A. Hedvall, *Z. Anorg. Allg. Chem.* 61 (1924) 135.
- [24] (a) H. Forestier, R. Lille, *Comp. Rend.* 204 (1937), p. 265, 1254;
(b) H. Forestier, R. Lille, *Comp. Rend.* 208 (1939) 891.
- [25] H. Forestier, M. Daire, *Akad. Der Wiss. Lit.* 7 (1966) 705.
- [26] C.G. Nestler, A. Faust, B. Kampfe, D. Lange, *Kristall Technik* 9 (1974) k57.
- [27] S. Starke, *Z. Phys. Chim.* 42B (1939) 159.
- [28] V.J. Arkharov, V.N. Bogosluvsy, *F.S. Met, Metallov* 3 (1965) 254.
- [29] G. Fagherazzi, *Chem. Ind. (Milan)* 47 (1965) 75.
- [30] M.L. Garcia-Gonzalez, P. Grange, B. Delmon, *Proceeding of the 8th ISRS*, Göthenburg, June, 1976.
- [31] W. Koster, L. bangert, R. Hahn, *Arch. Eisenhüttenw.* 25 (1954) 569.
- [32] A.R. Rosenfield, *Nature* 196 (1962) 1083.
- [33] P. Barrand, G.M. Leak, *Nature* 198 (1963) 279.
- [34] R. Schrader, W. Vogelsberger, *Z. Chim.* 9 (1969) 354.
- [35] M. Schneider, C.E. Beaulieu, *Mem. Sci. Rev. Metall.* 65 (1968) 869.
- [36] B. Gillot, J. Tyranowicz, A. Rousset, *Mater. Res. Bull.* 10 (1975) 775.
- [37] Behar, Collongues, *C.R. Acad. Sci.* 244 (1957) 617.
- [38] J. Szekely, J.W. Evans, H.Y. Sohn, *Gas–Solid Reactions*, Academic press, New York, 1976, p. 115, 232.
- [39] A. Ortega, *Thermochim. Acta* 284 (1996) 379.